Journal of
MATERIALS RESEARCH

Segregation in the $MgO–MgAl_2O_4$ system processed from nitrate precursors

Tania Bhatia,[a] K. Chattopadhyay, and Vikram Jayaram
Center for Advanced Study, Department of Metallurgy, Indian Institute of Science, Bangalore, 560012, India

(Received 12 June 1998; accepted 26 April 1999)

The occurrence of segregation and its influence on microstructural and phase evolution have been studied in $MgO–MgAl_2O_4$ powders synthesized by thermal decomposition of aqueous nitrate precursors. When the nitrate solutions of Mg and Al were spray-pyrolyzed on a substrate held at 673 or 573 K, homogeneous mixed oxides were produced. Spraying and drying the nitrate solutions at 473 K resulted in the formation of compositionally inhomogeneous, segregated oxide mixtures. It is suggested that segregation in the dried powders was caused by the difference in solubility of the individual nitrate salts in water which caused Mg-rich and Al-rich salts to precipitate during dehydration of the solutions. The occurrence of segregation in the powders sprayed at 473 K and not 573 or 673 K is ascribed to the sluggish rate at which the early stages of decomposition occurred during which the cations segregated. The phase evolution in segregated and segregation-free $MgO–MgAl_2O_4$ powders has been compared. The distinguishing feature of the segregated powders was the appearance of stoichiometric periclase grain dimensions in excess of 0.3 μm at temperatures as low as 973 K. By comparison, the segregation-free powders displayed broad diffraction peaks corresponding to fine-grained and nonstoichiometric periclase. The grain size was in the range 5–30 nm at temperatures up to 1173 K. The key to obtaining fine-grained periclase was the ability to synthesize (Mg Al)O solid solutions with the rock salt structure. In the temperature range 973–1173 K, spinel grain size varied from 5 to 40 nm irrespective of its composition and did not appear to be influenced by segregation.

I. INTRODUCTION

The usefulness of liquid precursor pyrolysis as a technique to study metastable effects in ceramics was illustrated by Wefers and Bell[1] who showed that a variety of metastable phases of Al_2O_3 could be produced on thermal decomposition of $Al(OH)_3$. More recently, metastability of products synthesized through pyrolysis of liquid precursors has been studied in several systems.[2–6] In a recent review, Levi[7] has explained the thermodynamics of metastability accessed through the pyrolysis of inorganic precursors. One of the most attractive features about the techniques involving pyrolysis is the low temperature ($T/T_m < 0.5$, where T/T_m is the homologous temperature) at which it is possible to synthesize metastable and nanophase materials. The work assumes importance from the recent finding of high degrees of compaction at low temperatures that have been obtained in amorphous and nanomaterials synthesized by thermal decomposition techniques.[8,9]

Processing multicomponent systems by thermal decomposition techniques often suffers from the problem of segregation, which results in compositional heterogeneity in the powders (or whiskers or thin films). If salts precipitate from the precursor solution before pyrolysis, the subsequent decomposition process yields regions of different compositions. An example of this has recently been obtained in $Y_2O_3–ZrO_2$ system.[5] Segregation depends on the nature of the precursor and is observed after the decomposition of the mixture of precursor salts and salt solutions. In contrast, a single-source precursor (for example produced by cohydrolysis) often yields a homogeneous product after thermal decomposition.[10] Segregation also depends on the actual process adopted for decomposition and the variation of solubility of the precursors with temperature. Thus a systematic study of the segregation behavior is essential for the development of

[a] Address all correspondence to this author.
Present address: Department of Metallurgy and Materials Engineering, Institute of Materials Science, Box U-136, University of Connecticut, Storrs, Connecticut 06269-3136.

the process based on thermal decomposition. In this article, we report the results of a study of the influence of prior segregation on the phase selection and evolution in thermally decomposed $MgO–MgAl_2O_4$ synthesized from nitrate precursors. In particular, we compare the results on thermally decomposed powders obtained on drying nitrate solutions with that of spray pyrolyzed products. The two cases correspond to situations representing the presence and absence of segregation. The choice of the system is dictated primarily by the availability of thermodynamic data.[4,11–12]

II. EXPERIMENTAL DETAILS

A. Thermal decomposition and characterization

Precalibrated aluminum nitrate [$Al(NO_3)_3 \cdot -xH_2O$] and magnesium nitrate hexahydrate [$Mg(NO_3)_2 6H_2O$] were mixed in double-distilled deionized water in the ratio required to yield MgO–20, 30, 40, and 50 mol% Al_2O_3. The solutions were subsequently dried at 473 K on a borosilicate evaporating dish. The salt solutions were also spray pyrolyzed on a borosilicate dish that was maintained at 673 and 573 K. Details of the spray pyrolysis technique used have also been discussed in Ref. 4. The powders obtained on thermal decomposition (both sprayed and dried) were heat treated at temperatures ranging between 973–1373 K in a platinum crucible, and the resulting phases were identified with x-ray diffraction (Huber Guinier diffractometer model 642) with Cu K_α radiation. The samples were also characterized by gravimetry using a CAHN thermogravimetric analyzer (TG 171).

B. Methods used in x-ray analysis

Because periclase and spinel are both cubic and their lattice parameters are in the ratio ≈1:2, the distinction between phases is difficult to make when the x-ray diffraction (XRD) peaks are broad. The presence or absence of the periclase peaks is especially difficult to establish because a spinel reflection is close to every periclase reflection. The problem is exacerbated when solid solution formation occurs because this reduces the separation between the two sets of peaks caused by lattice parameter shifts. The criteria for identification of the phases have been discussed in considerable detail in an earlier article[4] and are briefly: (i) splitting of the $(200)_p/(400)_s$ and $(220)_p/(440)_s$ peaks + strong $(311)_s$ peak → spinel and periclase present; (ii) no splitting of the $(200)_p/(400)_s$ and $(220)_p/(440)_s$ peaks + strong $(311)_s$ peak → single phase spinel; (iii) no splitting of the $(200)_p/(400)_s$ and $(220)_p/(440)_s$ peaks + weak or nonexistent $(111)_p/(311)_s$ peak → single phase periclase. Slow scan XRD data were used to calculated the exact peak positions. The data were fit to a Lorentzian function of the type:

$$I = K_1/[K_2{}^2 + (\theta - \theta_o)^2] + K_b \quad (1)$$

where, K_1, K_2, and K_b and θ_o were constants determined by regression analysis, I is the diffracted intensity that was measured at a scattering angle of θ. On the basis of the regression, the exact position of the peak is θ_o and the lattice parameter is calculated after accounting for the instrumental correction. K_b represents the background noise of the x-rays and was considered a constant for the calculations in a particular range of θ (typically 3–4°). In fact, θ_o remained the same even when the background was considered to vary linearly with diffraction angle, θ.

The composition of periclase and spinel is calculated on the basis of the lattice parameter shifts. Applicability of Vegard's law is assumed. For spinel, the variation in the lattice parameter between γ–Al_2O_3 ($a = 0.790$ nm) and stoichiometric $MgAl_2O_4$ ($a = 0.80831$ nm) is represented as:

$$a = 0.82662 - 0.03662y \quad (2)$$

where, y is the mole fraction of Al_2O_3 in the spinel phase. Estimation of the composition of periclase from its lattice parameter is based on the data available from previous work of Alper *et al.*[13] The variation in lattice parameter of periclase with composition is given by:

$$a = 0.4212 - 0.0276y \quad (3)$$

Both Eqs. (2) and (3) have proved successful in explaining earlier results reported on spray pyrolyzed powders and have been discussed in detail in Ref. 4.

The grain size t has been determined with Scherrer's formula[14,15]

$$t = K\lambda/\beta\cos\theta_o \quad (4)$$

where β is the full width at half-maximum (FWHM) and is given by $\beta = 4K_2$—instrumental broadening (estimated by running coarse-grained MgO as standard). K is known the shape factor and usually takes the value of about 0.9. Because Scherrer's formula gives an approximate value, K in the calculations in this study has been approximated at 1.0.

When an asymmetry of the peaks was present, the data could not be fitted to a single Lorentzian function. The data were then fitted to a sum of two Lorentizians:

$$I = K1/[K2^2 + (\theta - \theta_{o1})^2] + K3/[K4^2 + (\theta - \theta_{o2})^2] + K_b \quad (5)$$

The peak positions for the two peaks then were θ_{o1} and θ_{o2}. K2 and K4 were taken to be the measure of the individual peak widths.

III. RESULTS

A typical thermogram of the dried 20 mol% Al_2O_3 powders is shown in Fig. 1. Weight loss below the drying temperature of 473 K is expected to arise from reversible moisture absorption during storage. The samples reach a constant weight between 673 and 773 K. Thus little or no

volatile materials is remaining in the samples after heat treatments above 873 K. The effect of heat treatment on phase evolution in $MgO–MgAl_2O_4$ powders that were prepared by drying the nitrate solutions with composition of 50, 40, 30, and 20 mol% Al_2O_3 are shown in Figs. 2–5. The results are summarized in Table I(a), which lists the phases present in these materials as identified by XRD.

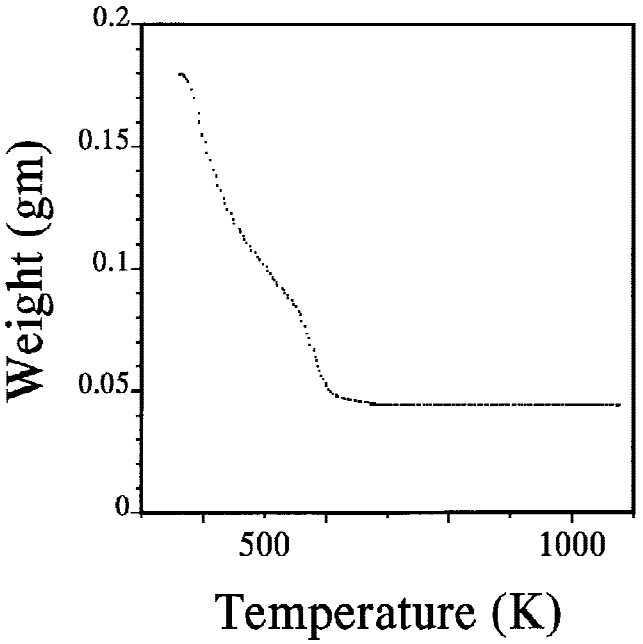

FIG. 1. TGA curve obtained from powders with composition MgO–20 mol% Al_2O_3 dried at 473 K.

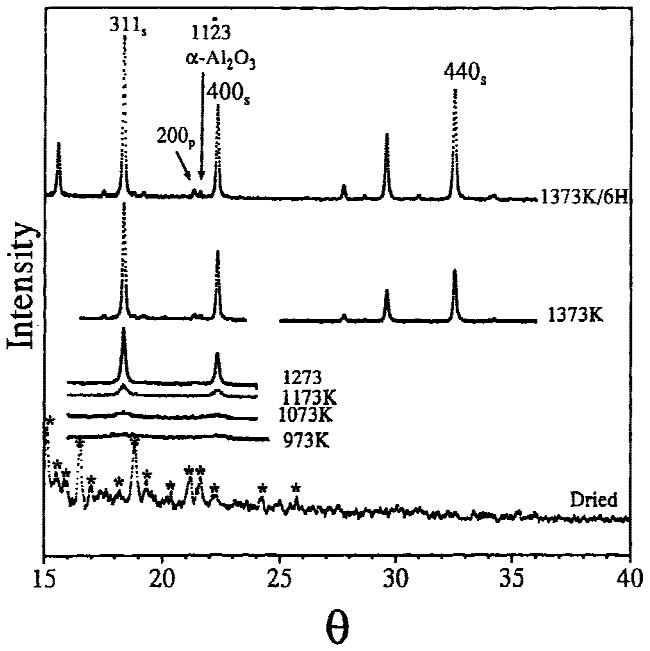

FIG. 2. Effect of heat treatment on MgO–50 mol% Al_2O_3 prepared by drying nitrate precursors at 473 K.

The as-dried powders contained unidentifiable peaks in all the compositions and have been marked "*" in XRD plots (Figs. 2–5). Heat treatment in the temperature range 623–673 K yielded x-ray patterns typical of non-crystalline products. Because these unidentified phases (marked "*") did not exist above 673 K, they are presumed to be complex hydrated nitrates.

In the 50 mol% Al_2O_3 composition, powders synthesized by drying nitrate solutions decomposed by 673 K and yielded amorphous powders. This is followed by crystallization of spinel which starts at 973 K. Weak peaks of periclase and corundum ($\alpha–Al_2O_3$) are observed in the dried powders after heat treatment at 1373 K (Fig. 2).

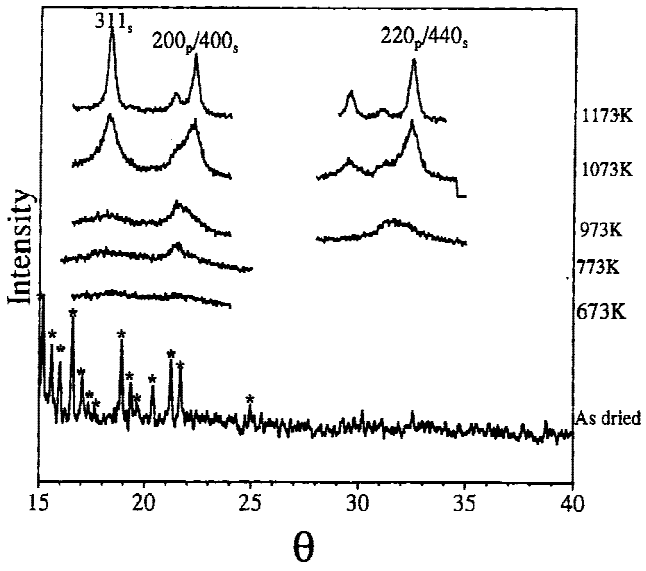

FIG. 3. Effect of heat treatment on MgO–40 mol% Al_2O_3 prepared by drying nitrate precursors at 473 K.

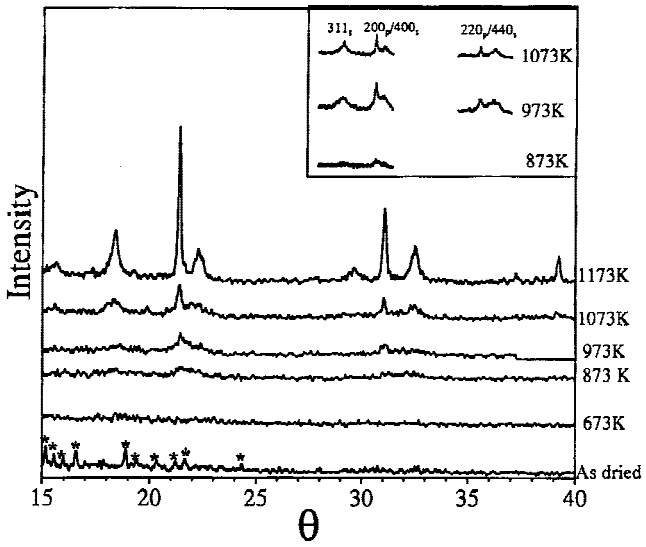

FIG. 4. Effect of heat treatment on MgO–30 mol% Al_2O_3 prepared by drying nitrate precursors at 473 K.

After drying at 473 K, the 40 mol% powders contained unidentifiable phases similar to the 50% powders (Fig. 3). After heat treatment at 973 K, the x-ray diffractograms of these powders show a broad and somewhat asymmetric peak corresponding to the $200_p/400_s$ reflection. The constituent phases are believed to be predominantly periclase with a small amount of poorly crystallized spinel. After heat treatment at 1073 K, the dominant phase is spinel with small amounts of periclase which is concluded from the shoulder on the 400_s peak. After heat treatment at 1173 K, the resultant phases were identified to be fine-grained spinel and periclase.

The dried solutions of MgO–30 and 20 mol% Al_2O_3 decomposed into a noncrystalline phase around 673 and 623 K, respectively (Figs. 4 and 5). In the 30 mol% Al_2O_3 powders, the x-ray patterns after the 973 K heat treatment show sharp peaks corresponding to periclase which begin to appear along with broad spinel peaks. The x-ray diffractograms of samples after heat treatments at 1073 and 1173 K show sharp periclase and relatively broader spinel peaks. The diffractograms of the heat-treated 20 mol% Al_2O_3 powders show sharp periclase peaks at temperatures of 673 K and above. Broad spinel peaks appear in the diffractogram only after heat treatment at 1073 K/1 h (as is clear from the inset in Fig. 5). X-ray diffractograms after heat treatment of powders synthesized by spraying solutions with 20 mol% Al_2O_3 at 473 and 573 K is shown in Figs. 6(a) and 6(b), respectively.

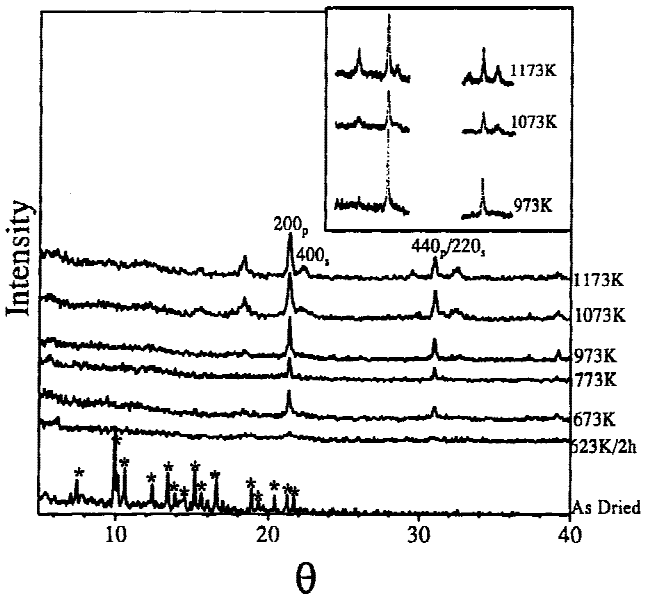

FIG. 5. Effect of heat treatment on MgO–20 mol% Al_2O_3 prepared by drying nitrate precursors at 473 K.

For ease of comparison between solutions that have been dried at 473 K and solutions that have been sprayed at 673 K, Fig. 7 has been reproduced from Ref. 4. It illustrates the effect of heat treatment on powders prepared by spray pyrolyzing nitrate precursors at 673 K. A list of the phases obtained on heat treatment of the spray-pyrolyzed powders is given in Table I(b). Tables II to V summarizes the composition and grain sizes (as calculated using Scherrer's formula) of the phases obtained in the pyrolyzed powders and in the dried powders.

In the spray-pyrolyzed powders (Fig. 7) with composition MgO–50 mol% Al_2O_3, spinel nucleates at 973 K, and the only phase seen in these powders is spinel even after heat treatments up to 1373 K. In the other compo-

TABLE I(b). Phases obtained in $MgO–MgAl_2O_4$ processed by spray pyrolysis of nitrate precursors at 673 K and subsequent heat treatment.

Heat treatment	20% Al_2O_3	30% Al_2O_3	40% Al_2O_3	50% Al_2O_3
973/1H	P	P	P	S
1073/1H	P + S	P + S	S	S
1173/1H	P + S	P + S	S + P[a]	S

P: periclase; S: spinel.
[a]Very small amounts.

TABLE I(a). Phases obtained in $MgO–MgAl_2O_4$ processed by drying of nitrate precursors at 473 K and subsequent heat treatment.

Heat treatment	20% Al_2O_3	30% Al_2O_3	40% Al_2O_3	50% Al_2O_3
As dried	Undecomposed salts	Undecomposed salts	Undecomposed salts	Undecomposed salts
623/2H	A	A	…	…
673/1H	P	A	A	A
773/1H	P	…	P	…
873/1H	…	P	P	…
973/1H	P + S[a]	P + S[a]	P + S[a]	S
1073/1H	P + S	P + S	S + P[a]	S
1173/1H	P + S	P + S	S + P	S
1273/1H	…	…	…	S
1373/1H	…	…	…	S + P + C
1373/6H	…	…	…	S + P + C

A: amorphous; B: periclase; S: spinel; C: corundum.
[a]Very small amounts.

sitions (20–40 mol% Al_2O_3), the phase present at 973 K is periclase. In the 20 and 30 mol% Al_2O_3 powders, a two-phase mixture of periclase and spinel is observed at 1073 K. As the powders are heated to 1173 K, the compositions of these two phases (as illustrated by shifts in XRD peaks) and their volume fractions change (Fig. 7 and Tables III and IV). In the MgO–40 mol% Al_2O_3, at 973 K the phase present is periclase, at 1073 K it is spinel, and at 1173 K the phases present are periclase and spinel.

IV. DISCUSSION

The dried MgO–50 mol% Al_2O_3 powders contain spinel along with periclase and corundum after heat treatment above 1273 K. The phase diagram predicts the line compound $MgAl_2O_4$ at the 50% composition. The phase diagram also clearly indicates that spinel supersaturated with MgO when heated to a high temperature would result in MgO (periclase) and spinel ($MgAl_2O_4$).[11] The presence of a homogeneous spinel phase with a composition of 50% Al_2O_3 would not result in MgO or corundum on heating up to the melting point. When MgO-rich spinel is heated, it precipitates MgO, and its composition shifts to that of stoichiometric spinel ($MgAl_2O_4$). Similarly $\alpha–Al_2O_3$ results from the decomposition of an Al_2O_3-rich spinel. The presence of periclase and $\alpha–Al_2O_3$ with spinel in materials containing 50 mol% Al_2O_3 implies that there were regions of nonstoichiometry in the dried powders. This is a clear indication of segregation during processing in powders with average composition 50 mol% Al_2O_3.

From Table II it may be noted that the composition of spinel in dried 50 mol% Al_2O_3 powders heat treated at 973 K is 34% Al_2O_3. Therefore, it is surmised that Al-rich $MgAl_2O_4$ crystallizes at a higher temperature than MgO-rich $MgAl_2O_4$ because there does not appear to be any contribution of the alumina-rich phases in the lattice

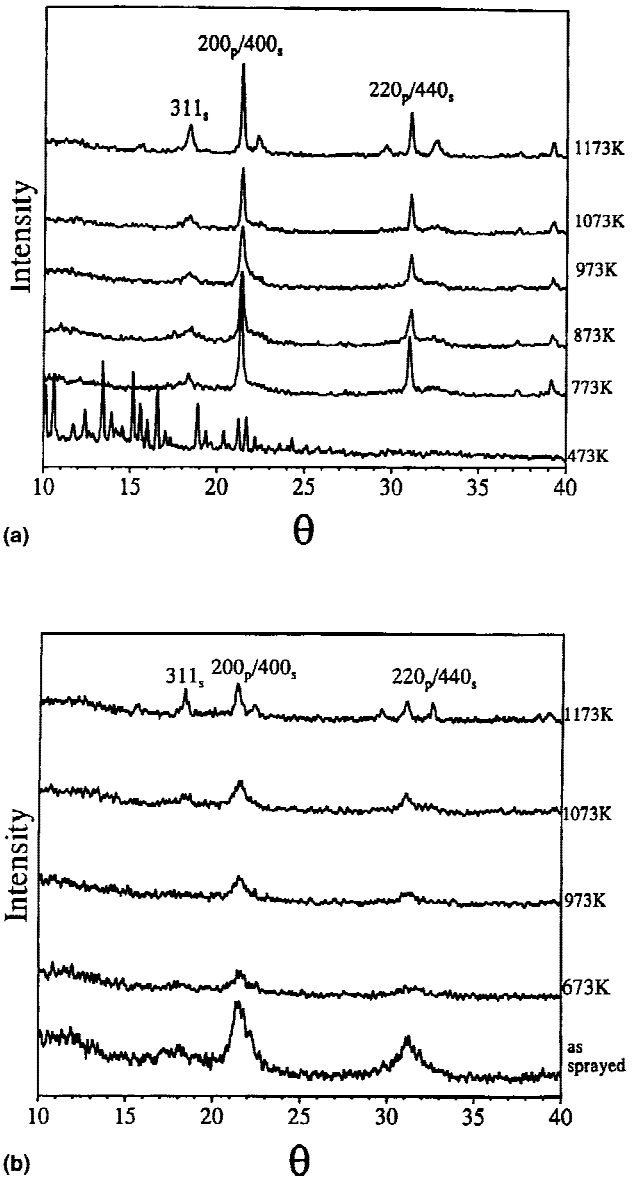

FIG. 6. Effect of heat treatment on MgO–20 mol% Al_2O_3 prepared by spraying nitrate precursors at (a) 473 K and (b) 573 K.

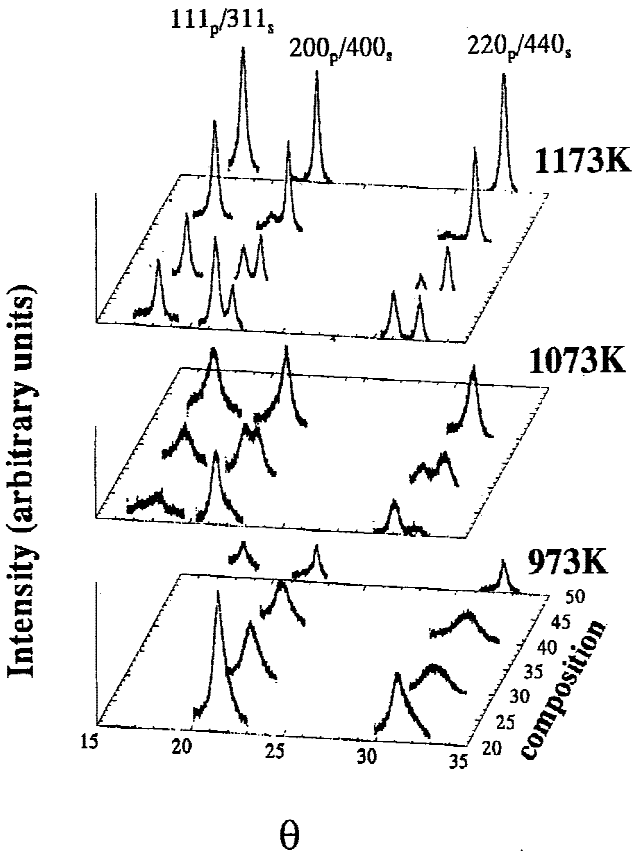

FIG. 7. Composite diffraction pattern that depicts the effect of heat treatment on spray pyrolyzed MgO–$MgAl_2O_4$; these show the phases present as a function of composition and temperature of heat treatment.

parameter. The occurrence of MgO and α–Al_2O_3 confirms that the dried powders with average composition of 50 mol Al_2O_3 which originally crystallizes as spinel at 973 K, was compositionally inhomogeneous with actual compositions greater and less than 50 mol% Al_2O_3.

In contrast to powders prepared by drying, the powders prepared by spraying at 673 K do not show the presence of periclase or α–Al_2O_3 (Fig. 7, Table II, and Ref. 4). The powders in the as-sprayed condition show a noncrystalline XRD pattern. When these powders are

TABLE II. Comparison between phases detected on heat treating dried powders and sprayed powders in MgO–50 mol% Al_2O_3. The numbers in the parentheses denote the composition of the phase (% Al_2O_3 content) deduced from its lattice parameter.

Heat treatment	Lattice parameter in dried sample (nm)		Lattice parameter in sprayed sample (nm)[4]		Grain size in dried sample (nm)		Grain size in sprayed sample (nm)[4]	
	Spinel	Periclase	Spinel	Periclase	Spinel	Periclase	Spinel	Periclase
973K/1H	0.814 (34%)	Not detected	0.8092 (48%)	Not detected	8	Not detected	19	Not detected
1173K/1H	0.8089 (48%)	Not detected	0.8083 (50%)	Not detected	34	…[a]	23	Not detected
1273K/1H	0.8089 (48%)	Not detected	…	Not detected	>300	…[a]	…	…
1373K/1H	0.8088 (49%)	0.4224	…	0.04224	>300	…[a]	…	Not detected
1373K/6H	0.8084 (50)	0.4225	…	0.4225	>300	…[a]	…	…

[a]XRD peak too weak for accurate determination of peak width.

TABLE III. Comparison between phases detected on heat treating dried powders and sprayed powders in MgO–20 mol% Al_2O_3. The numbers in the parentheses denote the composition of the phase (% Al_2O_3 content) deduced from its lattice parameter.

Heat treatment	Lattice parameter in dried sample (nm)		Lattice parameter in sprayed sample (nm)[4]		Grain size in dried sample (nm)		Grain size in sprayed sample (nm)[4]	
	Spinel	Periclase	Spinel	Periclase	Spinel	Periclase	Spinel	Periclase
973K/1H	…[a]	0.4214 (0.7%)	Not detected	0.418 (8.7%)	Not detected	>300	Not detected	5.5
1073K/1H	0.8147 (33%)	0.4210 (0)	0.8132 (37%)	0.4203 (3%)	18	>300	7.5	10
1173K/1H	0.8118 (40%)	0.4213 (0.4%)	0.8089 (48%)	0.4209 (1%)	42	>300	20	14.5

[a]XRD peak too weak for accurate determination of lattice parameter.

TABLE IV. Comparison between phases detected on heat treating dried powders and sprayed powders in MgO–30 mol% Al_2O_3. The numbers in the parentheses denote the composition of the phase (% Al_2O_3 content) deduced from its lattice parameter.

Heat treatment	Lattice parameter in dried sample (nm)		Lattice parameter in sprayed sample (nm)[4]		Grain size in dried sample (nm)		Grain size in sprayed sample (nm)[4]	
	Spinel	Periclase	Spinel	Periclase	Spinel	Periclase	Spinel	Periclase
973K/1H	0.8158 (30)	0.4215 (0%)	Not detected	0.4141 (26%)	9	30	Not detected	3.5
1073K/1H	0.8125 (39%)	0.42140 (0%)	0.8122 (39%)	0.41840 (10%)	11	>300	8	5.5
1173K/1H	0.8104 (44%)	0.4214 (0%)	0.8091 (48%)	0.4192 (7%)	25	>300	19.5	12

TABLE V. Comparison between phases detected on heat treating dried powders and sprayed powders in MgO–40 mol% Al_2O_3. The numbers in the parenthesis denote the composition of the phase (% Al_2O_3 content) deduced from its lattice parameter.

Heat treatment	Lattice parameter in dried sample (nm)		Lattice parameter in sprayed sample (nm)[4]		Grain size in dried sample (nm)		Grain size in sprayed sample (nm)[4]	
	Spinel	Periclase	Spinel	Periclase	Spinel	Periclase	Spinel	Periclase
973K/1H	0.8131 (37%)	0.417 (15%)	Not detected	0.4108 (38%)	8	5	Not detected	4
1073K/1H	0.8108 (33%)	0.417[a] (15%)	0.8129 (37%)	Not detected	8.5	14	9	Not detected
1173K/1H	0.8095 (47%)	0.4217 (2%)	0.8092 (48%)	0.419[a] (7%)	35.5	10	20.5	20

[a]Peaks were too weak to obtain a reasonable fit for lattice parameter calculations.

heated to higher temperatures, they yield single-phase spinel with no traces of periclase at any of the temperatures. This suggests that segregation does not occur in the powders spray pyrolyzed at 673 K.

Having established that segregation does occur when nitrate solutions are dried at 473 K, it is interesting to compare phase evolution sequences in the segregated and nonsegregated powders in the composition range 20–40 mol% Al_2O_3. A noncrystalline diffraction pattern is observed in the 20 mol% Al_2O_3 powders dried at 473 K after heat treatment at 623 K for 2 h (Fig. 5). On further heat treatment, the x-ray diffractograms of these powders developed sharp peaks of periclase with broad peaks of spinel appearing above 973 K. Comparison of the breadth of the periclase peaks in the heat-treated samples after drying at 473 K and spraying at 673 K can be easily made by inspecting the peaks in Figs. 5 and 7. The figures clearly show that the periclase peaks in the dried samples are much sharper than those in sprayed samples, implying that the periclase in the dried powders is coarse grained. The grain sizes observed have been presented in Tables III–V. Evidence that segregation in the 20 mol% powders resulted in pure magnesia after the 973 K heat treatment is seen from the lattice parameter of the periclase that has been listed in Table III (a_{MgO} = 0.4212 nm). The magnesia peaks become stronger with increasing heat treatment temperature and the corresponding lattice parameter does not change. On the basis of the lattice parameter data, the spinel composition is found to be 33% Al_2O_3 at 1073 K, and it moves to 40% Al_2O_3 at 1173 K. Thus it is concluded that nonstoichiometric spinel forms in the Al_2O_3-rich regions in the dried samples (average composition: 20 mol% Al_2O_3) at 1073 K and the phase composition shifts toward that of stoichiometric $MgAl_2O_4$ with heat treatment.

The trends seen in the dried 30 mol% Al_2O_3 powders are the same as in the 20 mol% Al_2O_3 powders. In contrast to the powders prepared by spraying at 673 K (Fig. 7), dried powders heat treated at 973 K display a sharp spike corresponding to pure magnesia, which intensifies on heating. The compositions deduced from the lattice parameters and grain sizes of the phases after different heat treatments are listed in Table IV.

The phase evolution in dried powders with composition of 40 mol% Al_2O_3 is more complicated than the 20 and 30 mol% Al_2O_3 compositions. The distinct sharp periclase peaks are not seen in this case. In nonsegregated (and spray pyrolyzed) powders of 40 mol% Al_2O_3, heat treatment at 973 K resulted in periclase, which transformed to spinel at 1073 K (Fig. 7). It has been established on the basis of x-ray lattice parameter data that the transformation occurs in a partitionless manner.[4] The diffraction maxima at each temperature, in conjunction with the criteria used in phase identification described earlier, were consistent with the presence of single phase with 40% Al_2O_3 composition, periclase at 973 K and spinel at 1073 K (Table V). Equilibrium partitioning to yield periclase and 50–50 spinel as predicted by the phase diagram began at 1173 K. In the case of powders prepared by drying, the predominant phase is periclase with very small amounts of spinel at 973 K (Fig. 3). The phase identification as periclase and spinel in the dried powders heat treated at 973 K has been made on the basis of asymmetry of the 200_p and 220_p peaks. The lattice parameter of the phases (listed in Table V) has been calculated by fitting the peaks to two Lorentzians as explained in section IIB. After heat treatment at 1073 K, the predominant phase is spinel with very small amounts of periclase. This is evidenced by the reversal in intensities of the spinel and periclase peaks and the appearance of a strong 311_s peak at 1073 K (Fig. 3). The presence of two phases in the 1073 K heat-treated samples is clear in the splitting of the $220_p/440_s$ doublet. The following phase evolution sequence has been surmised on the basis of the sequence already known for nonsegregated powders.[4] On the basis of thermodynamic and kinetic arguments and experimental data, it has been demonstrated (in powders prepared by spraying on to a substrate at 673 K) that in a competition between spinel and periclase, crystallization of periclase is preferred in compositions up to 40 mol% Al_2O_3. Therefore it is concluded that in the 40 mol% dried powders heat treated at 973 K, regions with composition close to 50 mol% Al_2O_3–nucleated spinel and other regions nucleated periclase. This implies that the amount of spinel would be much less than periclase and explains the absence of the 311_s and asymmetry of the 200_p in the x-ray diffractograms (Fig. 3). On heat treatment to 1073 K, the compositions close to 40 mol% transformed to spinel massively, while the periclase solid solutions with compositions close to about 30 mol% Al_2O_3 precipitated out spinel.

The basic difference between the x-ray diffractograms seen in the segregation-free powders and in the segregated powders lies in the sharp peaks of pure magnesia seen in the segregated powders (Figs. 4 and 5). The formation of a solid solution of periclase [(Al, Mg) O] appears to render it resistant to coarsening as is reflected in the grain sizes of periclase in the spray-pyrolyzed and dried powders (Tables III and IV). Because of the distinctness of the sharp periclase peaks, segregation can be most unmistakably established in the 20–30 mol% Al_2O_3 compositions unlike in the 40 mol% Al_2O_3, where the phase evolution sequence is more complicated and the 50 mol% Al_2O_3 compositions where the periclase and α–Al_2O_3 peaks are very weak.

Spray pyrolysis experiments were carried out for the 20 mol% Al_2O_3 solutions by maintaining the substrate at 473 and 573 K. Results obtained are shown in Figs. 6(a) and 6(b). On the basis of the sharp periclase peaks pres-

ent [Fig. 6(a)], it is evident that spraying on a substrate at 473 K could not prevent the occurrence of segregation. The powders synthesized by spraying at 573 K appear to be free from segregation. This is concluded from the formation of fine-grained (Al, Mg) O solid solutions which is evidenced in the broad diffraction peaks [Fig. 6(b)].

The process of precursor pyrolysis could be divided into two main events, namely, drying and decomposition. Consequently, there are two ways in which segregation could occur: (i) the precipitation of salts in the solvent (water) before complete drying and (ii) the precipitation of nitrates (and therefore oxides) during decomposition of the salt.

During the drying experiments, the solutions are heated slowly. It is believed that segregation occurs during the dehydration step because of the difference in the solubility of Al-nitrate (6.37 g/ml) and Mg-nitrate (1.25 g/ml) in water. As the water evaporates, the solutions get concentrated and Mg-rich nitrates precipitate, leaving Al-rich salts in the solution. The Mg-rich and Al-rich regions subsequently decompose to result in a final inhomogeneous oxide mixture.

Drying the solutions allows ample time for the salts to precipitate. However, segregation occurs even when powders are prepared by spraying the solution on a substrate at 473 K [Fig. 6 (a)] during which the heating rate experienced by droplets is at least two orders of magnitude higher than during drying. Also, segregation is avoided by spraying on a hot substrate maintained at 573 K [Fig. 6 (b)]. The heating rates experienced by the droplets at 473 and 573 K are likely to be of the same order of magnitude. Because precipitation of precursor salts is unlikely in the spraying experiments because of the high heating rates, it is surmised that the decomposition step is also important in deciding the occurrence of segregation. Thermogravimetric studies on the powders synthesized by drying (Fig. 1) show that out of a total weight loss of 60% above 473 K, the powders lost only 35% of their weight between 473 and 573 K (the remaining 25% was lost up to approximately 680 K). This implies that the powders sprayed at 573 K are not completely decomposed. The observation of segregation by spraying at 473 K and not at 573 K leads to the conclusion that the rate at which precursors are heated from 473–573 K plays an important role in deciding the final homogeneity of the powders. Although spraying at 573 K results in a modest increase in the heating rate up to 473 K, the reduction in the time spent beyond 473 K is more important in determining the occurrence of segregation. This is because the decomposition that occurs between 473–573 K takes place more slowly during holding at 473 K (on the substrate at 473 K) than when the substrate is at 573 K. In the powders synthesized by spraying at 673 K, the heating above 473 K is faster (than when the substrate is at 573 K) and the product is segregation-free. Because the powders sprayed at 573 and 673 K are free from segregation, it is concluded that the early stages of decomposition should take place fast enough to prevent the segregation of cations in the final product. It is also concluded that the later stages of decomposition do not affect segregation.

It is interesting to note that in the entire range of compositions, the spinel peaks in both dried and sprayed samples treated up to 1073 K are broad and independent of segregation in the system. The width of the periclase peaks appears to depend on its composition. It is seen that pure magnesia is not fine grained and coarsens rapidly, whereas spinel and alumina-rich solid solutions of magnesia appear to resist coarsening. Because fine spinel precipitates are common to both the segregated and nonsegregated powders, it is clear that pinning of grain boundaries by fine second-phase particles is not the cause for the difference in coarsening behavior of the rock salt phase (MgO).

One explanation for the difference in coarsening behavior of nonstoichiometric periclase is the occurrence of compositional inhomogeneity in the supersaturated periclase across grain boundaries. The occurrence of such grain boundary segregation effects is likely to reduce the grain boundary mobility if the solute concentration difference between the grain interior and the boundary is maintained during migration. However, we are unable to make a definite conclusion in this regard on the basis of the experimental results.

The contrasting coarsening behavior in segregated and segregation-free powders could also be ascribed to the formation of (Mg, Al) O solutions with different defect concentrations. The concentration of constitutional vacancies in periclase varies from 0% at pure MgO to 25% in case of solid solutions containing 50 mol% Al_2O_3. The difference between pure MgO and Al-rich MgO could be attributed to the development of short-range order (brought about by a high concentration of vacancies) in the Al_2O_3–rich MgO solid solution found in segregation-free powders. This implies that alumina-rich periclase solid solutions are not completely random. The prospect of finding such nonrandom solid solutions is not entirely unexpected and can be related to the similarities in the two end structures of the pseudobinary $MgO–MgAl_2O_4$. Both periclase (MgO) and spinel ($MgAl_2O_4$) have a face-centered-cubic packing of oxygen ions and differ in the way the cations are arranged. In MgO, all the octahedral interstices are occupied by cations, and aliovalent additions of Al^{3+} ions bring about vacancies in the cation sites. In $MgAl_2O_4$ one eighth of the tetrahedral interstices and half the octahedral interstices are occupied by cations. Nonstoichiometry in the MgO-rich solid solutions of $MgAl_2O_4$ is accommodated by the presence of Mg^{2+} ions in the vacant octahedral sites.[11,16] It has been postulated that a defect spinel (formed under rapid solidifi-

cation conditions) could transform to the equilibrium phases by going through structures intermediate between spinel and periclase.[12] Suggestions of such intermediate metastable structures have also been made on the basis of experiments on the amorphization of spinal by heavy ion bombarbment at cryogenic temperatures.[17–19] In this study, it is believed that the slower coarsening rates in alumina-rich solid solutions of periclase are caused by the formation of such structures, which implies longer jump distances for the atoms and the vacancies because all the cationic sites are not energetically equivalent.

It is seen from our observations that nonstoichiometry in the spinel phase does not affect its grain size. This implies that charged defects in periclase have a much more pronounced effect on coarsening rate than charged defects in spinel. This could be a manifestation of the capacity of spinel to accommodate large deviations from stoichiometry on both sides of the line compound $MgAl_2O_4$. In addition, the coarsening rate of stoichiometric spinel, as seen from XRD patterns of unsegregated 50% alumina, is also lower than that of pure periclase, thereby possibly reflecting the longer time needed for the cooperative diffusion of both cationic species.

V. SUMMARY

Segregation and its effect on phase and microstructural evolution in the $MgO–MgAl_2O_4$ system have been studied. The oxides are produced by thermal decomposition of aqueous nitrate solutions. The occurrence of segregation which results in inhomogeneous oxide mixtures is determined by two factors: (i) the rate at which the dehydration of nitrate solutions occur and (ii) the rate at which the early stages of the precursor decomposition is accomplished. To avoid segregation, the multicomponent precursor solutions need to be heated rapidly to avoid precipitation of precursor salts in the solvent. It is also essential to heat the precursors rapidly during the initial stages of salt decomposition.

A distinct difference in the phase evolution between segregated and nonsegregated powders was observed. Segregation during processing, resulted in the occurrence of periclase with sharp x-ray peaks indicating a coarse-grained nature of pure MgO. In comparison, in the segregation-free powders, the XRD peaks of periclase were broad and they corresponded to fine-grained and nonstoichiometric periclase. The key to obtaining a fine-grained microstructure is to be able to synthesize (MgAl)O solid solutions with the rock salt structure. The resistance of such solid solutions to coarsening is possibly due to the formation of a large concentration of point defects that could show a tendency to order. Spinel is fine grained (<50 nm) and shows broad diffraction peaks up to 1173 K irrespective of its composition.

ACKNOWLEDGMENTS

Financial support for this work was provided by a grant from the Department of Science and Technology, Government of India. Additional support for the project was provided by a grant through United States–India funds [NSF Grant No. INT-9633039]. One of the authors (T.B.) would like to acknowledge the Department of Atomic Energy, Government of India, for financial assistance extended to her through the Dr. K.S. Krishnan Fellowship Program.

REFERENCES

1. K. Wefers and G. M. Bell, *Oxides and Hydroxides of Aluminum,* Technical Paper No. 19 (Alcoa Research Laboratories, Alcoa Center, PA, 1972) as quoted in ref 2.
2. M.L. Balmer, F.F. Lange, and C.G. Levi, J. Am. Ceram. Soc. **77,** 2069 (1994).
3. M.L. Balmer, Ph.D. Thesis, University of California, Santa Barbara (1993).
4. T. Bhatia, K. Chattopadhyay, and V. Jayaram, Mater. Sci. Eng. A **A226–228,** 930 (1997).
5. V. Jayaram, M. DeGraef, and C.G. Levi, Acta Metall. **42,** 1829 (1994).
6. A.D. Polli, F.F. Lange, C.G. Levi, and J. Mayer, J. Am. Ceram. Soc. **79,** 1745 (1996).
7. C.G. Levi, Acta Mater **46,** 787 (1998).
8. R.S. Mishra, V. Jayaram, B. Majumdar, C.E. Lesher, and A.K. Mukherjee, Colloids and Surfaces **A133,** 25 (1998).
9. A.S. Gandhi, V. Jayaram, and A.H. Chokshi, Mater Sci. Forum **243–245,** 227s (1997).
10. M. Nyman, J. Caruso, and M.J. Hampden-Smith, J. Am. Ceram. Soc. **80,** 1231 (1997).
11. B. Hallstedt, J. Am. Ceram. Soc. **75,** 1497 (1992).
12. T. Bhatia, K. Chattopadhyay, and V. Jayaram, (unpublished).
13. A.M. Alper, R.N. McNally, P.H. Ribbe, and R.C. Doman, J. Am. Ceram. Soc. **45,** 263 (1962).
14. R. Jenkins in *Reviews in Minerology,* edited by D.L. Bish and J.E. Post, (Minerological Society of America) Vol. 20, p. 66.
15. B.D. Cullity, *Elements of X-ray Diffraction,* 2nd ed. (Addison-Wesley Publishing Company, 1978).
16. V.S. Stubican and R. Roy, J. Phys. Chem. Solids **26,** 1293 (1965).
17. N. Yu, K. E. Sickafus, and M. Nastasi, Phil. Mag. Lett. **70,** 235 (1994).
18. S.P. Chen, Y. Yan, J.D. Gale, R.W. Grimes, R. Devanathan, K.E. Sickafus, N. Yu, and M. Nastasi, Phil. Mag. Lett. **73,** 51 (1996).
19. R. Devanathan, K.E. Sickafus, N. Yu, and M. Nastasi, Phil. Mag. Lett. **72,** 155 (1995).